

# Studying Frame-Resistant Steel Structures under near Field Ground Motion

S. A. Hashemi, A. Khoshraftar

**Abstract**—This paper presents the influence of the vertical seismic component on the non-linear dynamics analysis of three different structures. The subject structures were analyzed and designed according to recent codes. This paper considers three types of buildings: 5-, 10-, and 15-story buildings. The non-linear dynamics analysis of the structures with assuming elastic-perfectly-plastic behavior was performed using RAM PERFORM-3D software; the horizontal component was taken into consideration with and without the incorporation of the corresponding vertical component. Dynamic responses obtained for the horizontal component acting alone were compared with those obtained from the simultaneous application of both seismic components. The results show that the effect of the vertical component of ground motion may increase the axial load significantly in the interior columns and, consequently, the stories. The plastic mechanisms would be changed. The P-Delta effect is expected to increase. The punching base plate shear of the columns should be considered. Moreover, the vertical component increases the input energy when the structures exhibit inelastic behavior and are taller.

**Keywords**—Inelastic behavior, non-linear dynamic analysis, steel structure, vertical component.

## I. INTRODUCTION

THE study of earthquake motions observed in recent earthquakes indicates that the vertical ground acceleration could be more than a horizontal component [1], [2]. The vertical component increases in near-source earthquakes [3], such as the Northridge earthquake of January 1994, the Kobe earthquake of January 1995 and, the Bam earthquake of December 2003. According to reports of the Northridge earthquake, the vertical component of the earthquake could have had an important effect [4].

For numerical evaluation, earthquake motions are generally represented by three components. The peak ground acceleration of the vertical component is usually smaller than those of the two horizontal components. Therefore, most building codes with earthquake provisions require that an equivalent lateral load due to horizontal ground motion be used in simplified empirical approaches which directly contradicts the current codal provision that assumes the value of the vertical ground motion to be 1/2 to 2/3 of the horizontal component [5], [6]. The effect of the vertical component is considered indirectly. Obviously, if the vertical component is much stronger than that which considered normal, then the

simplified code approaches may underestimate the seismic load and the structure will not perform as intended.

According to the studies performed on the influence of the vertical ground acceleration on structures, the vertical component may increase the axial load [7]-[9]. In most of these researches the effects of vertical component of earthquake in near-fault areas was considered as very extensive in both compression and tension, and can lead to serious uplift problems [4].

By studying 5-, 10- and 15-story buildings, the seismic responses have been calculated using the RAM PERFORM-3D program, which can apply the three components of ground motions simultaneously. Analyses have been performed once considering and once without considering the vertical component of ground motion to decipher the effect of vertical excitation in combination with horizontal excitations. The increasing axial force in the middle columns and the increasing input energy are presented. Graphs depicting the columns' axial force versus axial strain, the time history of the yield ratio, the hysteresis of the story axial force versus story vertical deformation, the time history of the input energy, the hysteresis of the story shear versus story drift, the maximum story drift and the story shear and, final displacement of the structures have been plotted for the study.

## II. ANALYSIS PROCEDURE

In this analysis of steel structures, the three most common assumptions for the material behavior were elastic-perfectly-plastic behavior, isotropic strain hardening [10], and contemplation of the problem's complexity within the context of typical engineering practices. In this study, the material nonlinearity of steel is considered to be elastic-perfectly-plastic.

Time history analysis was used in this study because the response spectral method cannot describe the response of a structure when in the near-field of an earthquake.

When an axial force is present in a box-section under bending action, the plastic moment changes from the value  $M_p$ , at zero axial force, to a reduced value  $M_{p,r}$ , at the same time the neutral axis moves away from the centroidal axis.

Suppose that the box-section in Fig. 1 (a) becomes fully plastic under the combined action of an axial thrust  $P$  applied through the centroid and a bending moment  $M_{p,rx}$  applied in the plane of the web. At lower values of  $P$ , the neutral axis lies between the flanges with the stress distribution shown in Fig. 1 (b), but at higher values, the neutral axis moves into a flange, as shown in Fig. 2.

S. A. Hashemi is with the Department of Civil Engineering, Ahvaz Branch, Islamic Azad University, Ahvaz, Iran (e-mail: hashemi@iauahvaz.ac.ir).

A. Khoshraftar is with the Department of Civil Engineering, Ahvaz Branch, Islamic Azad University, Ahvaz, Iran (corresponding author to provide phone: +989126203757; e-mail: Khoshraftar@iauahvaz.ac.ir).

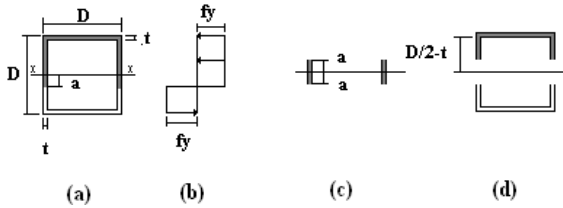


Fig. 1 The effect of the axial force on the plastic moment of a box-section when the neutral axis moves in the web

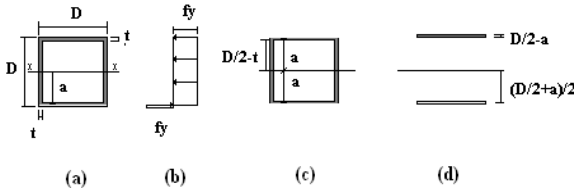


Fig. 2 The effect of the axial force on the plastic moment of a box-section when the neutral axis moves in the flange

The relationship between the reduced plastic moment  $M_{prx}$  and the thrust  $P$  may be obtained by dividing the cross-section into a symmetrical core area and two equal outer areas. The core area is subjected entirely to compressive stresses (Figs. 1 (c) and 2 (c)); one of the two outer areas will be under tension, and the other will be under compression (Figs. 1 (d) and 2 (d)). The core areas depicted in Figs. 1 (c) and 2 (c) may be considered to resist the axial force  $P$ , while the remaining outer areas in Figs. 1 (d) and 2 (d) resist the moment  $M_{pr}$ . If  $a$  is the distance of the neutral axis from the centroidal axis, then Fig. 1 applies when  $a < (D/2-t)$  and Fig. 2 when  $(D/2-t) < a < D/2$ , where  $D$  is the depth of the section and  $t$  are the flange and web thicknesses.

As Fig. 1 (c) represents the resistance to the thrust  $P$ , then

$$P = 4atf_y \quad (1)$$

Moreover, as Fig. 1 (d) represents the resistance to the reduced plastic moment  $M_{prx}$ , then

$$M_{pr} = M_p - 2t \left[ \frac{(2a)^2}{4} \right] f_y \quad (2)$$

The value of  $M_{pr}$  is obtained by noting that the reduction of the plastic moment below the value  $M_p$  (when no axial force is present) is represented by the loss of the plastic moment of the web area in Fig. 1 (c).

If the section becomes plastic under an axial thrust only, the value of the thrust would be  $P_p = Af_y$ , where  $A$  is the area of the cross-section. This thrust  $P_p$  is known as the *squash load* representing the load that would be sustained by a very short member failing by pure axial compressive deformation. If the ratio  $P/P_p$  (the *squash load ratio*) is denoted by  $n$ , then from (1),

$$a = P/(4tf_y) = nP_p/(4tf_y) = nA/(4t)$$

Substituting this value of  $a$  into (2), it follows that

$$M_{pr} = M_p - \left( \frac{A^2}{8t} \right) n^2 f_y \quad (3)$$

This formula applies until the axial thrust becomes so high that the neutral axis ceases to lie in the web.

Turning now to the case when the neutral axis is in a flange (Fig. 2), it can be seen that the core area (Fig. 2 (c)) is the area left after removing two flange areas each with width  $D$  and thickness  $(D/2-a)$  from the original section of area  $A$ . Hence,

$$P = [A - 2 \left( \frac{D}{2} - a \right) D] f_y \quad (4)$$

The moment of resistance  $M_{prx}$  is derived from the two flange areas in Fig. 2 (d). The centroids of these areas are at a distance  $[a + 0.5(D/2 - a)]$ , i.e.,  $.5(D/2 + a)$  from the centroidal axis. Hence,

$$M_{prx} = 2 \left[ \left( \frac{D}{2} - a \right) D f_y \right] \left[ \frac{1}{2} \left( \frac{D}{2} + a \right) \right] \quad (5)$$

Substituting  $P = nAf_y$  in (4), gives  $a = .5[D - (1-n)A/D]$ , whence from (5),

$$M_{prx} = \frac{A^2 f_y}{4D} (1-n) \left[ \frac{2D^2}{A} + n - 1 \right] \quad (6)$$

These relationships, (3), and (6), obtained for a box-section are similar to those obtained for an I-section [11]. As steel columns (with box-section) under combined axial compression and bending stress shall be evaluated using Equation, it has the following form:

$$\left| \frac{P_U}{P_{U0}} \right| + \left| \frac{M_U}{1.18M_{U0}} \right| = 1 \quad (7)$$

where  $P$  is the axial force;  $M$  is the bending moment; and  $P_{U0}$  and  $M_{U0}$  are the axial strength capacity and the flexural strength capacity, respectively.

### III. DESCRIPTION OF STRUCTURES AND EARTHQUAKES

Three structures representing different dynamic characteristics are considered in this study: a five-, ten- and fifteen-story steel structure, all shown in Fig. 3. They represent short, intermediate and tall buildings, respectively. The geometry of these three structures and their plans, which show the location of columns, are shown in Fig. 3, and their member sizes are given in Table I. The story height for these structures is a constant 3 m, and the width of each bay is 5 m. All three structures are assumed to have rigid connections, and are assumed to be located in Tehran. These three structures were subjected to the five strong-motion earthquakes identified in Table II.

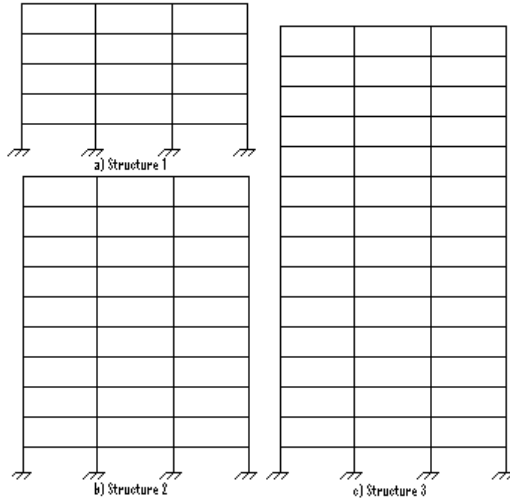


Fig. 3 Three steel structures

TABLE I  
MEMBER SIZES

Structure	Story	Columns	Girders
1	1-3	Box,280,280,20	IPE400
	4-5	Box,240,240,20	IPE360
2	1-3	Box,340,340,20	IPE400
	4-5	Box,280,280,20	IPE400
	6-7	Box,280,280,20	IPE360
3	8-10	Box,220,220,20	IPE360
	1-4	Box,380,380,20	IPE500
	5	Box,320,320,20	IPE500
	6-8	Box,320,320,20	IPE450
	9-10	Box,260,260,20	IPE450
	11-12	Box,260,260,20	IPE400
	13-15	Box,200,200,20	IPE400

TABLE II  
STRONG-MOTION EARTHQUAKES

Earthquake	Station	Acceleration		
		PGAH1	PGAH2	PGAV
Bam	Bam, Farmandari	0.7896g	0.6337g	1.0118g
Northridge	Tarzana, Cedar Hill nurseri	0.9903g	1.7794g	1.048g
Kobe	Kobe, Takarazu	0.6934g	0.6935g	0.4335g
Manjil	Manjil, Abbar	0.5991g	0.4992g	0.5033g
Tabas	Tabas	0.8358g	0.8517g	0.6885g

IV. RESULTS AND DISCUSSION

A. Effect of the Vertical Component on Axial Force

The effect of the vertical component on the variation of the axial force in the middle columns is greater than that in the other columns because the loading surface of the middle columns is larger than that of the other columns. The increasing axial force in the middle columns is presented in Table III. Consequently, the P-Delta effect is expected to increase and punching base plate shear of the columns should be considered [12], [13].

TABLE III  
INCREASE IN AXIAL FORCE IN MIDDLE COLUMNS (%)

Structure	Analysis	Northridge	Bam	Tabas	Kobe	Manjil
5-Story	0, V	97%	55%	24%	25%	43%
	90, V	73%	51%	15%	20%	40%
	3D	103%	56%	---	---	---
10-Story	0, V	101%	34%	30%	25%	36%
	90, V	91%	29%	26%	23%	29%
	3D	101%	35%	---	---	---
15-Story	0, V	100%	33%	24%	25%	33%
	90, V	100%	35%	26%	20%	30%
	3D	95%	23%	---	---	---

B. Effect of the Vertical Component on the Hysteresis of Axial Force-Strain in Columns

The effect of the vertical component on the hysteresis of the axial force-strain in columns deserves attention. In some cases, the vertical component causes the column to yield earlier than in the case in which the effect of the vertical component is not considered consequently the plastic mechanisms would be changed, but the effect of the vertical component on bending moments in columns is negligible. Figs. 4-9 show, respectively, the time history of the yield ratio and the hysteresis of the axial force-strain in columns.

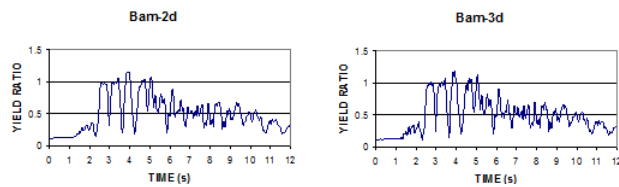


Fig. 4 Time history of yield ratio for the middle column in the first story of a 5-story building

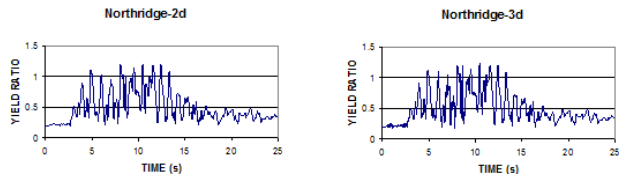


Fig. 5 Time history of yield ratio for the middle column in the first story of a 10-story building

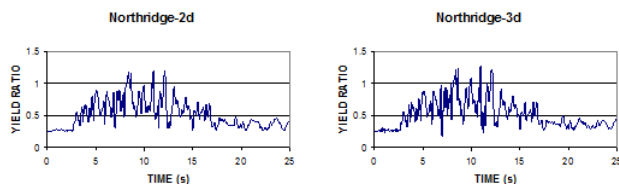


Fig. 6 Time history of yield ratio for the middle column in the first story of a 15-story building

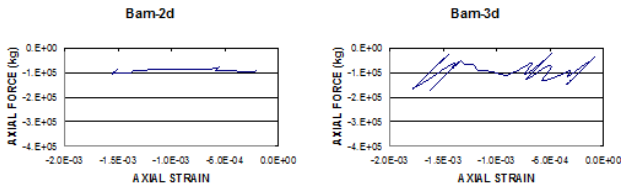


Fig. 7 Hysteresis of axial force-strain for the middle column in the first story of a 5-story building

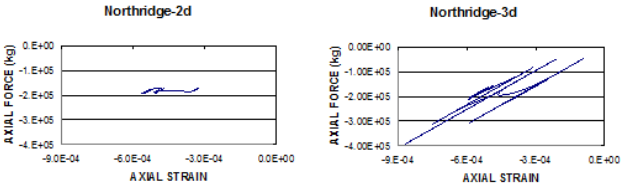


Fig. 8 Hysteresis of axial force-strain for the middle column in the first story of a 10-story building

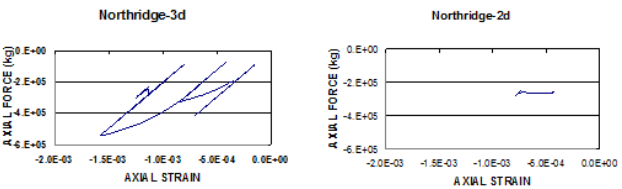


Fig. 9 Hysteresis of axial force-strain for the middle column in first story of a 15-story building

*C. Effect of the Vertical Component on Axial Force in Stories*

The effect of the vertical component causes the stories' axial forces to increase up to twice their primary value. In the analysis conducted without the vertical component, the axial force in stories was constant. Fig. 10 shows the hysteresis of the axial force-vertical deformation stories.

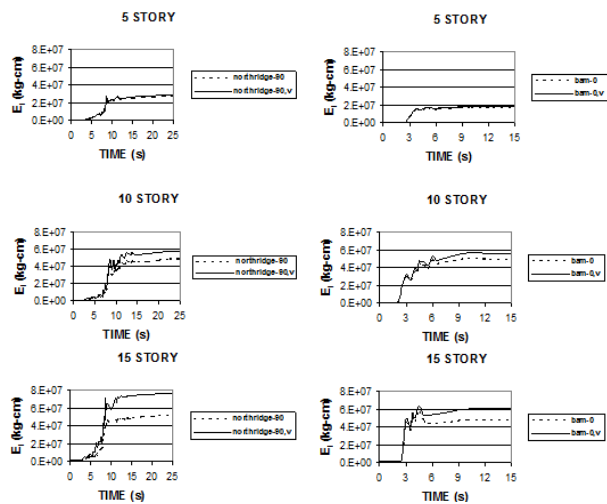


Fig. 10 Time history of input energy

*D. Effect of the Vertical Component on Input Energy*

An energy balance equation is determined by integrating the equation of motion with respect to the displacement,  $u$ .

$$\int_u m \ddot{u} du + \int_u c \dot{u} du + \int_u f_s du = - \int_u m \ddot{u}_g du \quad (8)$$

For (8),  $m$  is the mass,  $c$  is the coefficient of viscous damping,  $f_s$  is the restoring force,  $\ddot{u}_g$  is the ground acceleration, and  $u$ ,  $\dot{u}$  and  $\ddot{u}$  are the displacement, velocity, and acceleration of the mass, respectively.

It should be noted that the restoring force,  $f_s$ , represents the spring force of the inelastic system. From the left to the right side of (8), the first term is referred to as the kinetic energy  $E_K$ , the second term is the damping energy,  $E_D$ , and the third term represents the absorbed energy and consists of the elastic strain energy,  $E_S$ , and the inelastic hysteretic energy,  $E_H$ . The term on the right-hand side of (8), corresponds to the input energy of the ground motion,  $E_I$ , or the work done by the effective earthquake force,  $-m\ddot{u}_g$ . Hence, the energy balance equation can be expressed as [14],

$$E_K + E_D + E_S + E_H = E_I \quad (9)$$

When considering the vertical component of the ground motion, causing the input energy of the ground motion to increase. According to Fig. 10, the input energy increases when the structures exhibit inelastic behavior and are taller. The increasing percent of the input energy in the structures is presented in Table IV.

TABLE IV  
INCREASE IN INPUT ENERGY (%)

EI	5Story	10Story	15Story
Northridge 90, V	4%	18%	48%
Bam 0, V	6%	13%	25%
Kobe 0, V	0.3%	2%	5%
Manjil 90, V	11%	14%	18%
Tabas 0,V	7%	10%	16%

*E. Hysteretic of Shear Force-Story Drift*

To properly control the modeling and analysis of the structures using RAM PERFORM-3D software, one must be able to rely on the hysteresis of the shear force-story drift. Fig. 11 shows the stiffnesses of the stories. From the lower to upper stories, respectively, the effect of the vertical component on the hysteresis of the shear force versus story drift is negligible.

*F. Comparison between Static and Dynamic Shear Force*

The ratio  $D/S$  of the dynamic shear force relative to the static shear force in the stories of a structure is very different. Fig. 12 shows that the  $D/S$  ratios of the stories of tall buildings are very different from one another. Fig. 13 shows that the pattern of static loading in 10- and 15-story buildings is not related to code pattern, the true pattern in tall buildings according to the reverse  $S$  shape.

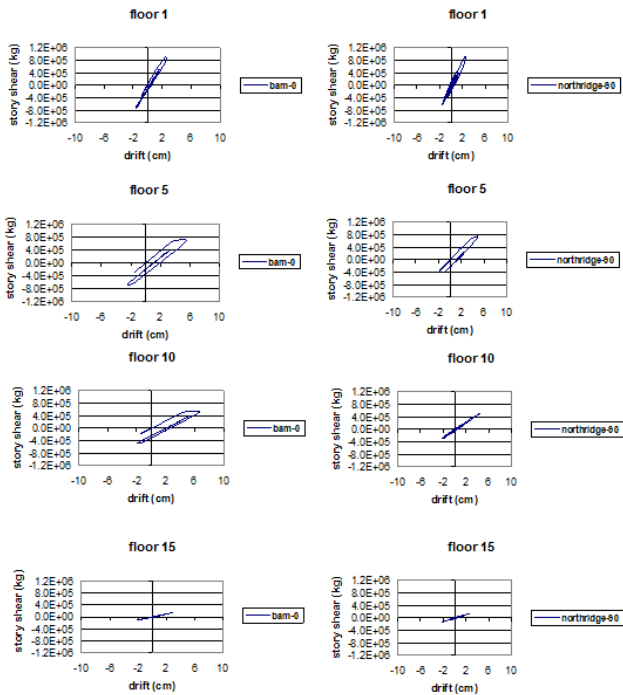


Fig. 11 Hysteresis of shear force versus story drift

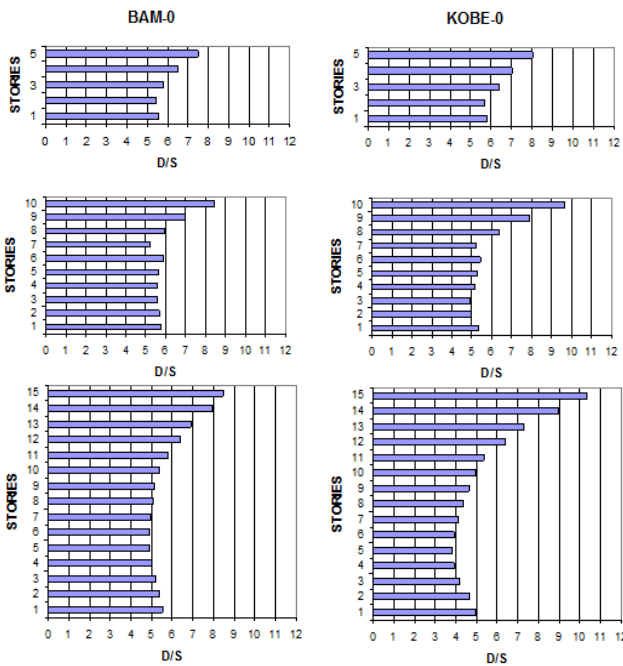


Fig. 12 The ratio of the dynamic shear force relative to static shear force in stories

*G. The Maximum Story Drift*

Fig. 14 shows that the maximum story drift often occurs in middle stories because the stiffness in these stories is less than that of the lower stories, and the yielding elements of middle stories are greater than those of upper stories. Also, Fig. 11 shows that the maximum story drift occurs in the middle story.

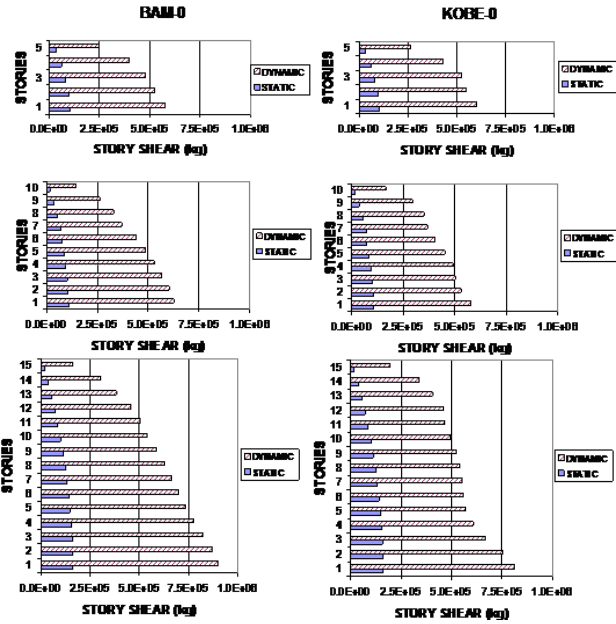


Fig. 13 Maximum dynamic shear force and static shear force in stories

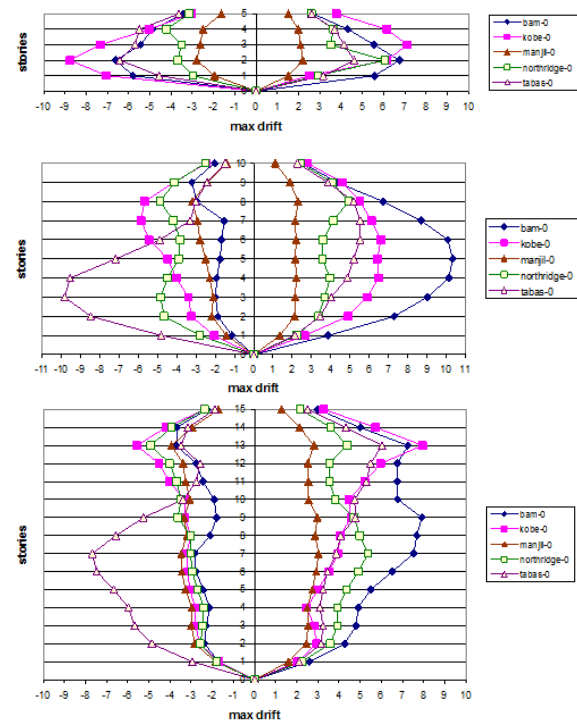


Fig. 14 Maximum story drift in structures

*H. The Final Displacement of Structures*

Fig. 15 shows that the final displacement shape of the structures in some of the earthquakes is the same as that of the first or second mode.

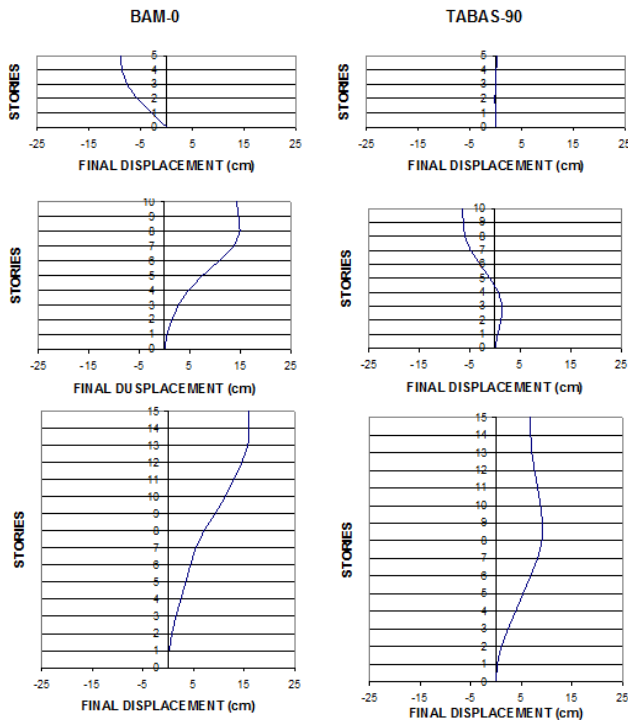


Fig. 15 Final displacement of structures

## V. CONCLUSION

Based on the numerical results of this study it can be concluded that:

- The effect of the vertical component of ground motion causes an increase in the axial force in middle columns and that the axial force in stories increases up to twice (~103%) its primary value; consequently, the P-Delta effect is expected to increase punching base plate shear of the columns should be considered.
- The effects of the vertical component on the bending moment in columns, story shear and drift are negligible.
- In some cases, the vertical component causes the column to yield earlier than in the case in which the effect of the vertical component is not considered consequently the plastic mechanisms would be changed.
- The vertical component of the ground motion causes the input energy to increase up to 48% when the structures exhibit inelastic behavior and are taller.
- According to the results, the pattern of static loading for tall buildings abiding by current codes is unsuitable.
- Often, the maximum story drift occurs in the middle stories.
- The final displacement shape of structures in some earthquakes adopted that of the first or second mode.

## REFERENCES

- [1] J. Despyrox, "Some lessons to be Draw from the El Asnam Earthquake of October10, 1980." *Proc. 8th World conference on Earthquake Engineering*, San Francisco, California, July 1984.

- [2] G. Warn, and A. Whittaker, "Vertical Earthquake Loads on Seismic Isolation Systems in Bridges." *J. Struct. Eng.*, 134(11), 1696-1704, 2008.
- [3] W. D. Iwan, "Near-Field Consideration in Specification of Seismic Design Motion for Structure", *Proc. of the 10th European conference on Earthquake Engineering*, Vienna, Austria, 28 August- 2 September 1994.
- [4] B. Hosseini Hashemi, and E. Abbassi, "Rational Suggestions for Vertical Component Requirement in 2800 Iranian Standard for Near-Fault Areas", *J. Seismol. Earthquake Eng.*, 10(4), 189-194, 2009.
- [5] C.G. Salmon, and J.E. Johnson, *Steel Structures: Design and Behavior, 4th ed. HarperCollins College*, New York, USA, 1996.
- [6] E. Kalkan, and P. Gülkan, "Empirical attenuation equations for vertical ground motion in Turkey", *Earthquake Spectra*, 20(3), 853-882, 2004.
- [7] A. Salazar, and A. Haldar, "Structural Responses Considering the Vertical Component of Earthquakes", *Computers and Structures*, 2000 74,131-145.
- [8] M. Hosseini, and M. Firoozi Nezamabadi, "A Study on the Effect of Vertical Ground Acceleration on the Seismic Response of Steel Building", *Proc. of the 13th WCEE*, Vancouver, B.C., Canada, August 2004.
- [9] S. G. Kim, C. J. Holub, and A. S. Elnashai, "Analytical Assessment of the Effect of Vertical Earthquake Motion on RC Bridge Piers", *J. Stru. Eng.*, 137 (2), 252-260, 2011.
- [10] O.R. Owen, and E. Hinton, *Finite Element in Plasticity: Theory and Practice. Pineridge Press*, Swansea, UK, 1982.
- [11] M. R. Horne, *Plastic Theory of Structures*, Nelson, London, UK, 1971.
- [12] E. Kalkan, and V. Graizer, "Multi-component ground motion response spectra for coupled horizontal, vertical, angular accelerations, and tilt", *ISET J. Earthquake Technol.*, 44 (1), 259-284, 2007.
- [13] E. B. Williamson, "Evaluation of Damage and P-D Effects for Systems under Earthquake Excitation", *J. Struct. Eng.*, 129(8), 1036-1046, 2003.
- [14] A. K. Chopra, *Dynamics of Structures: Theory and Applications to Earthquake Engineering*, Prentice Hall, Upper Saddle River, New Jersey, USA, 1995.



**Ali Khoshraftar** was born in Khorram Abad, Lorestan, Iran in September 20th, 1979. He received a Bachelor of Science degree in civil engineering with a major in structural engineering from Isfahan University of Technology in Isfahan, Iran in 2003. He completed a Master of Science degree in civil engineering with a major in structural engineering from Iran University of Science and Technology in Tehran, Iran in 2005. He is a PhD student at the Faculty of Civil Engineering, Islamic Azad University of Arak.

He was Head of Structural Department at general office of Khuzestan organization of schools from 2006 to 2009. Meanwhile, he was a Master Expert and Engineer of seismic vulnerability evaluation of school buildings from 2008 to 2009. He has been an Instructor in Civil Engineering Department of Islamic Azad University in Ahvaz, Iran since 2009. He became Associate Dean of Education in Engineering Department and Head of Construction Department of Civil Engineering Department of Islamic Azad University in Ahvaz, Iran since 2010. He published an article entitled "The effect of degradation on seismic damage of RC buildings" in 8th International Conference on Civil and Architecture Engineering, Cairo, Egypt in 2010, and published an article entitled "The evaluation of steel frame structures with viscoelastic dampers" in 2<sup>nd</sup> International Conference on Civil and Urban Engineering -ICCUE 2015, March 19-20, 2015, Florence, Italy. His research interests are Safety evaluation and retrofit of existing structures, Rehabilitation of structures and Durability and repair of concrete structures.

Mr. Khoshraftar is a member of Iranian Earthquake Engineering Association (IEEA), Iranian Society of Civil Engineers (ISCE) and Iranian Concrete Institute (ICI). He has a certificate in Earthquake Disaster Management from Asian Disaster Reduction Center (ADRC) in cooperation with Japan International Cooperation Agency (JICA). He also holds a Rehabilitation of Existing Structures certificate from Iranian Earthquake Engineering Association (IEEA).